

# Seasonality of runoff and precipitation regimes along transects in Peru and Austria

Maria M. Cárdenas Gaudry, Dieter Gutknecht, Juraj Parajka<sup>\*</sup>, Rui A.P. Perdigão, Günter Blöschl

Institute for Hydraulic and Water Resources Engineering, Vienna University of Technology, Karlsplatz 13/223, A-1040 Vienna, Austria.

<sup>\*</sup> Corresponding author. E-mail: parajka@hydro.tuwien.ac.at

**Abstract:** The aim of this study is to understand the seasonalities of runoff and precipitation and their controls along two transects in Peru and one transect in Austria. The analysis is based on daily precipitation data at 111 and 61 stations in Peru and Austria, respectively, and daily discharge data at 51 and 110 stations. The maximum Pardé coefficient is used to quantify the strength of the seasonalities of monthly precipitation and runoff. Circular statistics are used to quantify the seasonalities of annual maximum daily precipitation and annual maximum daily runoff. The results suggest that much larger spatial variation in seasonality in Peru is because of the large diversity in climate and topography. In the dry Peruvian lowlands of the North, the strength of the monthly runoff seasonality is smaller than that of precipitation due to a relatively short rainy period from January to March, catchment storage and the effect of upstream runoff contributions that are more uniform within the year. In the Peruvian highlands in the South, the strength of the monthly runoff seasonality is greater than that of precipitation, or similar, due to relatively little annual precipitation and rather uniform evaporation within the year. In the Austrian transect, the strength of the runoff seasonality is greater than that of precipitation due to the influence of snowmelt in April to June. The strength of monthly regime of precipitation and runoff controls the concentration of floods and extreme precipitation in Peruvian transects. The regions with strong monthly seasonality of runoff have also extreme events concentrated along the same time of the year and the occurrence of floods is mainly controlled by the seasonality of precipitation. In Austria, the monthly runoff maxima and floods occur in the same season in the Alps. In the lowlands, the flood seasonality is controlled mainly by summer extreme precipitation and its interplay with larger soil moisture.

The analyses of precipitation and runoff data along topographic gradients in Peru and Austria showed that, overall, in Peru the spatial variation in seasonality is much larger than in Austria. This is because of the larger diversity in climate and topography.

**Keywords:** Seasonality; Regime; Precipitation; Runoff; Floods; Austria; Peru; Transect; Pardé coefficient.

## INTRODUCTION

The runoff regime of catchments is a result of numerous interacting processes including the movement and phase change of water in the atmosphere and in the vegetation, on the land surface and in the soils. Investigating these processes is challenging because of their large spatial and temporal variability. One approach of exploiting this variability is comparative hydrology (Falkenmark and Chapman, 1989; Gaál et al., 2012) which aims at learning from the differences in different parts of the landscape to understand the process controls of runoff. This may help with building catchment classification schemes (Wagener et al., 2007), developing and selecting hydrologic model structures (Fenicia et al., 2013) and mapping of hydrological signatures for predictions in ungauged basins (Blöschl et al., 2013). One of the signatures used for identifying process controls is the seasonality of the runoff regime. There are numerous studies on the seasonality of monthly runoff (e.g. Bower et al., 2004; Gottschalk, 1985; Haines et al., 1988; Johnston and Shmagin, 2008; Pardé, 1947), but many of them examine the hydrological regime only over a single region (e.g. Molnar and Burlando, 2008; Petrow et al., 2007; Sauquet et al., 2008). The advantage of using large datasets crossing the borders of administrative and climate units has been pointed out by Gupta et al. (2014). While such studies are less common (see e.g. Dettinger and Diaz, 2000; Krasovskaia, 1995, 1996; Krasovskaia and Gottschalk, 2002; Parajka et al., 2010) there is renewed interest in them in connection with improving hydrological predictions under changing conditions (Montanari et al., 2013).

This paper explores the seasonalities of runoff and precipitation regimes in Peru and Austria. Seasonality assessments in Peru in the past focused mainly on the precipitation regime, its temporal variability and the impact of the El Niño Southern Oscillation (ENSO) signal on monthly and extreme precipitation. For example, Lagos et al. (2008) examined statistical relationships between monthly precipitation and sea surface temperature anomalies in Peru and delineated three El Niño precipitation regimes (North, Centre and South) in the Andean mountain region. Espinoza et al. (2009) found low rainfall seasonality in Ecuador, and a bimodal rainfall regime with peaks in April and October in the intra-Andean basins in Peru and the Amazon plain (at the border of Peru, Brazil and Colombia). Rau and Condom (2010) observed a marked seasonality in precipitation above 3000 m in Peru with maxima in January to March and minima in June to August. Lavado et al. (2012) investigated rainfall runoff variability and its trends in three Peruvian regions (Pacific, Amazonas and Titicaca basins). They found low correlations between monthly precipitation and runoff in some Pacific basins which they attributed to the effects of groundwater storage, glacier melt and anthropogenic activities such as water abstraction for irrigation, hydropower production and water supply. A global analysis of Dettinger and Diaz (2000) found that the lag times between the months of maximum precipitation and those of runoff vary smoothly from long delays in mountainous regions to relatively short delays in the lowlands.

In Austria, the seasonality of hydrological regimes was analyzed mainly in the context of flood producing processes (Merz

and Blöschl, 2003; Merz et al., 1999; Piock-Elena et al., 2000). For example, Merz and Blöschl (2003) identified and analyzed different types of causative mechanisms of floods by using the seasonality of maximum annual flood peaks as an indicator describing the timing of floods. Parajka et al. (2009) analyzed the differences in the climatic conditions, long-term hydrological regime and flood processes along a transect between Austria and Slovakia. Their results suggest that the seasonality of precipitation and runoff regimes is an important indicator of flood processes. It varies considerably in space as a result of the relative role of soil moisture, evaporation and snow processes. The differences in the seasonality between precipitation and runoff were found to be more pronounced in the lowland and hilly regions than in the mountains. Parajka et al. (2010) extended the seasonality analysis to the Alpine Carpathian range and demonstrated the important role of regional soil moisture.

The aim of this paper is to compare and examine the seasonalities of monthly and annual maximum daily precipitation and runoff across three transects in Peru and Austria. While one Peruvian transect represents latitudinal variability of climate, the other two transects represent the effect of topography in Peru and Austria. The main advantage of altitudinal transects is that altitude is expected to have strong effects on snow and evaporation processes as well as on the precipitation magnitudes which will facilitate identifying the controls. The selected transects show similar topographical variability, but cross different climate zones in the two countries which facilitate a comparative analysis. We believe that the assessment and comparison of hydrologic regimes in regions with such large gradients allows inferring more robust interpretations than by using results from a single region only.

## STUDY SITES, DATA AND METHODS

### Study Sites

The seasonality of the precipitation and runoff regimes and their controls are analysed for three transects in Peru and Austria (Fig. 1). Transect 1 extends from North to South along the west slope of the Andes from 3°S to 18.5°S in Peru (Fig. 1,

left). Transect 1 is the longest (1512 km) and represents large variations in the latitude, a large diversity of climate classes, and the influence of Pacific sea water currents or the Atlantic regime. Most of the catchments in Transect 1 drain to the Pacific Ocean with an exception in section km 250–320, 450–460 and 960–1330 that drain to the Atlantic (the Amazon basin).

Transect 2 cuts across the coastal plain and the Andes from Southwest to Northeast in Northern Peru (Fig. 1, centre). It extends from the coastal plain and depressions to the occidental mountain range and ends in the Andes Valleys. Transect 2 features differences in climate due to both altitudinal effects, and Pacific (km 0–130) and Atlantic (km 130–260) climatic regimes. Transect 3 cuts across the Eastern Alps in Austria from North to South extending from 48.5°N to 46.5°N (Fig. 1, right). It features differences in climate due to both altitudinal effects, and Atlantic and Mediterranean Sea climatic regimes. Transects 2 and 3 have a similar length of about 260 km.

### Data

The hydrological data used in this study are daily and monthly precipitation and discharge data from the period 1961–2010. Precipitation was observed at 111 and 61 climate stations in Peru and Austria, respectively (Fig. 1). The stations are situated at a wide range of elevations ranging from 1 to 4633 m a.s.l. in Peru, and from 308 to 1820 m a.s.l. in Austria. Mean monthly temperatures at the climate stations were used as a reference for discussing the runoff controls. Discharge data from 51 and 110 gauging stations in Peru and Austria were used, respectively. Catchment areas range from 6 to 14560 km<sup>2</sup>. All input data were carefully screened for errors and, where possible, the data were corrected. Otherwise they were removed from the data set. The final data set contains at least 10 years of data in the period 1961–2010. The average length of data series is for precipitation and discharge 28 and 22 years for Peru and 45 and 36 years for Austria, respectively. The stations were assigned to the axes of the transects on a nearest neighbour basis of their locations.

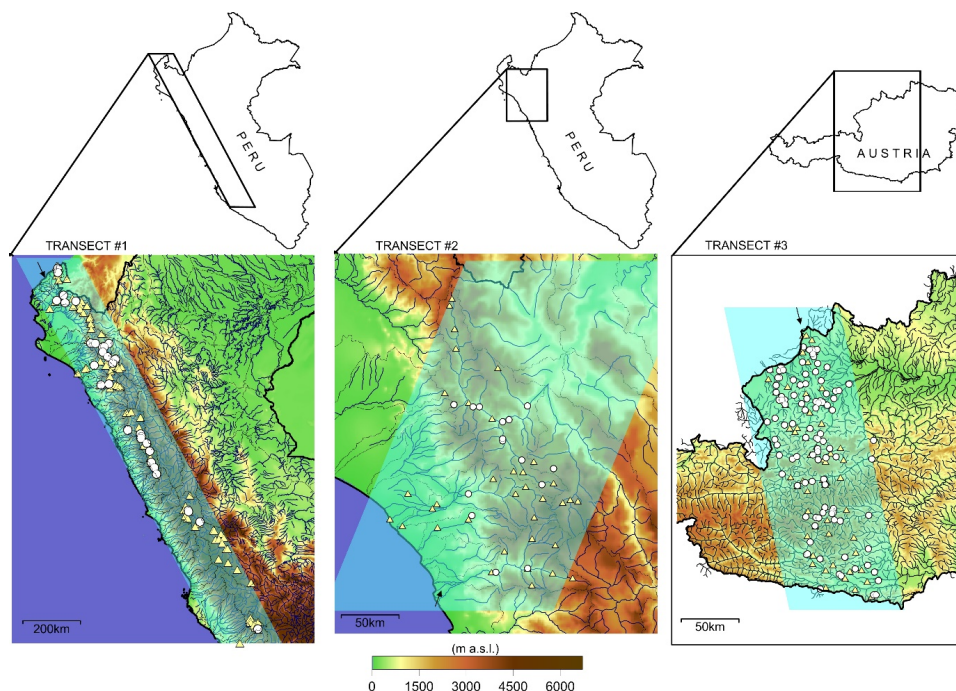


**Fig. 1.** Topography and rivers of Peru (left: Transects 1 and 2) and Austria (right: Transect 3), with location of precipitation (triangles) and runoff stations (circles) along the transects.

**Table 1.** Summary of climate stations and stream gauges used to illustrate the water balance in Figs. 2–4. Mean annual precipitation (MAP). Mean annual runoff depth (MAQ). Mean annual temperature (MAT).

ID in figures	Basin	Station	Altitude m a.s.l.	MAP (mm/yr)	MAQ (mm/yr)	MAT (°C)	Area (km <sup>2</sup> )
P1a, T1a	Chancay-Lambayeque	Tinajones	250	133		24	
P1b		Chugur	2750	1314			
Q1		Racarumi	250		399		2400
T1b		Rupahuasi	2850			11	
P2a,Q2a,T2a	Acari	Cecchapampa	3900	833	569	7	250
P2b,T2b	Ica	Malluchimpana	2500	116		16	
Q2b		La Achirana	420		110		2600
P3a	Zaña	Oyotun	200	201			
P3b		Udima	2300	986			
Q3		Batan	200		304		673
T3a		Station 4929	855			20	
T3b		Station 4930	2400			15	
P4	Chotano	Chota	2400	987			
Q4		Lajas	2125		960		356
T4		Chota	1610			16	
P5	Mattig	Mattighofen	455	1142			
Q5, T5		Jahrsdorf	380		340	8	447
P6,Q6,T6	Enns	Schladming	730	1014	1043	4	649

Table 1 gives a summary for selected climate stations and stream gauges used to illustrate the water balance in Figs. 2–4.

### Controls

The Köppen climate classification was used to identify the climate zones of the sites (Köppen, 1884; MINEDU, 2008). The following Köppen climate groups can be found in the transects (Köppen indices in brackets):

- Tropical savanna climate (Aw)
- Steppe climate (BS)
- Desert climate (BW)
- Temperate climate (C)
- Hemi-boreal climate with dry winter and warm summer (Dwb)
- Snow and glacier dominated mountain climate (E)

Peru should have a predominantly tropical climate with abundant rainfall, high temperatures and exuberant vegetation due to its geographical location. However, climate is affected by the presence of the Andes mountain range, the Humboldt Current and the South Pacific anticyclone which result in a more diverse climate (UNESCO, 2006). Sites located in the Pacific catchments in the North of Peru have Tropical savanna, steppe and desert climates. The other Pacific catchments have steppe and desert climates up to 2000 m a.s.l. Temperate climates with dry winters are found in the steppe and low Andean valleys. Temperate humid climates are found in the Austrian transect. Snow dominated climates occur in the highest parts of Transect 1 and much of Transect 3.

Lowest annual precipitation occurs at the Peruvian coast (0–500 m a.s.l.) with a mean annual precipitation (MAP) of 4–870 mm/yr. In the highlands (500–4633 m a.s.l.) the range of MAP is from 62 to 1466 mm/yr. MAP decreases from North to South. In the Austrian lowlands (330–500 m a.s.l.) MAP ranges from 809–1520 mm/yr and in the highlands (500–1820 m a.s.l.) from 750–1943 mm/yr. Mean annual temperatures vary from 19°C in the coastal plains of Peru to 9°C in the highlands, and from about 10°C in the Austrian lowlands to around –8°C in the highest parts of the Alps.

The Peruvian transects are affected by a range of air fluxes. In the North, the greatest single control on the annual cycle is

the meridional migration of the Inter-tropical Convergence Zone (ITCZ) (Poveda et al., 2006). The annual cycle of precipitation in the Peruvian Andes is related to the seasonal displacement of the South Pacific and South Atlantic anticyclones, the north-south seasonal displacement of the Intertropical Convergence Zone, humidity transport from the Amazon, and the formation of a center of high pressure in high levels of the atmosphere (Lagos et al., 2008).

The Austrian Transect 3 shows Zonal West influence of air masses in the North and centre, and Meridional Southeast and South influence in the South of the transect (Parajka et al., 2010).

### Seasonality analysis

The seasonality of the monthly precipitation and runoff regimes is evaluated by the index proposed by Pardé (1947). For each month of the year, an index  $Pk_i$  is estimated as:

$$Pk_i = \frac{12}{n} \sum_{j=1}^n \left( \frac{Q_{ij}}{\sum_{i=1}^{12} Q_{ij}} \right) \quad (1)$$

where  $Q_{ij}$  represents the mean monthly runoff (or precipitation) in month  $i$  and year  $j$ , and  $n$  is the record length in years. The  $Pk_i$  values range between 1 and 12, where  $Pk_i = 1$  represents a uniform (non-seasonal) distribution of mean monthly runoff (or precipitation) around the year, while  $Pk_i = 12$  indicates a very strong seasonality when all the runoff (or precipitation) occurs only in one month. The strength of runoff or precipitation seasonality  $Pk_{max}$  is defined here as the maximum value of  $Pk_i$ :

$$Pk_{max} = \max_i (Pk_i) \quad (2)$$

The month  $i_{max}$  in which the maximum occurs is also noted. In the following,  $Q-Pk_{max}$  and  $P-Pk_{max}$  refer to the maximum Pardé coefficients for runoff and precipitation, respectively.

The seasonalities of annual maxima of daily runoff and daily precipitation are estimated by circular statistics (e.g. Bayliss and Jones, 1993; Burn, 1997). The mean date and variability of occurrence of the extreme events represents an average position of particular event occurrences, which are plotted in polar coordinates on a unit circle. The position of the event occurrence on

a unit circle is defined by the angle:

$$\Theta_i = D_i \frac{2\pi}{365}, \quad i = 1, \dots, n \quad (3)$$

where  $D_i$  is expressed as day of the year ( $D_i = 1$  for January, 1<sup>st</sup>, and  $D_i = 365$  for December 31<sup>st</sup>).

The variability of the date of occurrence about the mean date is evaluated by the concentration index  $r$ , which represents the length of unit vector representing the mean date of runoff or precipitation events. The concentration index ranges from  $r = 0$  (no temporal concentration of extreme events around the year) to  $r = 1$  (all extreme events of precipitation or floods occur on the same day of the year) (see e.g. Parajka et al., 2009, 2010).

## RESULTS AND DISCUSSION

The results of the seasonality strengths of the monthly precipitation and runoff regimes along the three transects are presented in Figs. 2, 3 and 4. In each of the figures, the top panels show the long term water balance for two basins on the transect (see Table 1), i.e. monthly precipitation (triangles) and monthly runoff depths (circles) as well as monthly average air temperatures (squares). The middle panels show the  $Pk_{max}$  values of precipitation (full triangles) and of runoff (full circles) along the distance of the transects with the month  $i_{max}$  of  $Pk_{max}$  colour coded. The bottom panels show the median and maximum elevations of the transects.

### Seasonality of monthly precipitation and runoff along transects

The  $Pk_{max}$  - values of precipitation of Transect 1 (triangles in Fig. 2) are high (up to 5) in the North, decrease until km 800 and then increase again. The Pacific North of Transect 1 is influenced by the El Niño current with greater precipitation amounts than the Pacific-Central and southern part influenced by the Humboldt current, restricting the evaporation of the cold water and increasing the aridity of the region. The ITCZ influence for the austral autumn (Vera et al., 2000) is also evident in section km 0–95 (Tumbes basin) where precipitation peaks occur in February–March and  $P-Pk_{max}$  are somewhat smaller than around km 145–230. The sites with Atlantic influence of Transect 1 are controlled by the trade winds where precipitation maxima occur in January–March.

Mean annual precipitation decreases from North to South. Differences in elevation are the main reason for differences in MAP for the same location along the transect. Wet season precipitation in the lowlands is concentrated in three months, resulting in large seasonality strengths. In the highlands, precipitation is spread over more months, resulting in a smaller seasonality strength. Espinoza et al. (2009) studied the length of the dry season in the tropical Andes in Peru (highlands) and noted that 20% of the annual rainfall is registered from June to August. A similarly strong seasonality was found by Rau and Condom (2010) in the Peruvian Andes above 3000 m a.s.l. coinciding with km 603–803 and 960–1330 of Transect 1.

The timing of the runoff regime is similar in all basins, with runoff maxima mostly in March (Espinoza et al. 2009), coinciding with the time of  $Pk_{max}$  of precipitation. An exception are the Atlantic basins located in the Andes Valleys where maximum runoff occurs between March and May and maximum precipitation between December and April.

The trend of the maximum seasonality of runoff in Transect 1 (circles) follows basically the trend of the maximum

seasonality of precipitation with  $Q-Pk_{max}$  around 3.5 in the North, km 38–69 (Tumbes basin), a decrease towards the South until km 750 with values around 2 and then an increase to values around 4, at km 1480 (Acari basin). However, there are important differences between the seasonality of runoff and precipitation. In the North, the  $Q-Pk_{max}$  are smaller than those of precipitation while the opposite is the case in Central and Southern Peru.

To explain the differences between the seasonalities of precipitation and runoff it is useful to examine the water balance of two typical basins. Fig. 2 top left shows the water balance components of the Chancay-Lambayeque basin (km 400–438 of Transect 1) that drains into the Pacific Ocean with two typical precipitation stations within the basin.

Precipitation station P1a is located at the coast at 250 m a.s.l. and is under the influence of Pacific air fluxes. Precipitation station P1b is located in the Andes at 2750 m a.s.l. and is under the influence of Atlantic air fluxes. The maximum Pardé coefficient of precipitation decreases with increasing altitude. Discharge station Q1a is located at 250 m a.s.l. The runoff regime of Q1 is a composite of the Atlantic and Pacific influences. The Chancay-Lambayeque basin is an example where the runoff seasonality is smaller than the precipitation seasonality at the coast. This is because of catchment storage effects as well as the runoff contributions from higher parts of the catchment where the rainfall regime is more uniform.

The Ica and Acari basins (Fig. 2 top right), again draining into the Pacific Ocean, illustrate examples in the South where runoff seasonality is greater than precipitation seasonality, or similar. Precipitation station P2a and discharge station Q2a are located at 3900 m a.s.l. Precipitation station P2b is located at 2500 m a.s.l. and discharge station Q2b is located at 420 m a.s.l. In these catchments annual precipitation is relatively low. Rather uniform evaporation throughout the year results in losses that reduce the average annual runoff while leaving the amplitude (mm/month) of runoff similar. This then translates into  $Q-Pk_{max}$  that is larger than the  $P-Pk_{max}$  (Acari).

The  $Pk_{max}$  values of precipitation of Transect 2 (triangles in Fig. 3) strongly decrease with the distance from the coast from  $P-Pk_{max}$  5 to 1.3. Similar to precipitation, the maximum runoff seasonality decreases with the distance from the coast from  $Q-Pk_{max}$  3.2 to 1.4. However, the maximum Pardé coefficient of runoff is smaller than that of precipitation in the Southwest (Pacific and Atlantic influence) up to km 130. Conversely, the Pardé coefficient of runoff is greater than that of precipitation in the East, for example at km 135–140, where Q4 is greater than P4 (Atlantic influence).

The water balance components of the Zaña basin in Fig. 3 top left, again, help explain the seasonality. P3a and Q3 are located at the coast at 200 m a.s.l., and P3b in the Andes at 2300 m a.s.l. Q3 is affected by both storage and inflow from the headwaters with high precipitation seasonality, resulting in a runoff seasonality smaller than that of precipitation at the coast. In Chotano in the Northeast of Transect 2 (Fig. 3 top right) the role of upstream headwaters is small, similar to Acari. A rather uniform evaporation throughout the year results in a reduction of average annual runoff, and therefore a  $Q-Pk_{max}$  larger than  $P-Pk_{max}$ .

The  $Pk_{max}$  values of precipitation of Transect 3 (triangles in Fig. 4) slightly increase from the northern Alpine lowlands (mean  $P-Pk_{max}$  is 1.4) to the high Alps (mean  $P-Pk_{max}$  is 1.7) and in turn somewhat decrease as one moves to the Southern Pre-Alps (mean  $P-Pk_{max}$  is 1.5). The stronger seasonality in the Alps is due to orographic effects (Parajka et al., 2010).

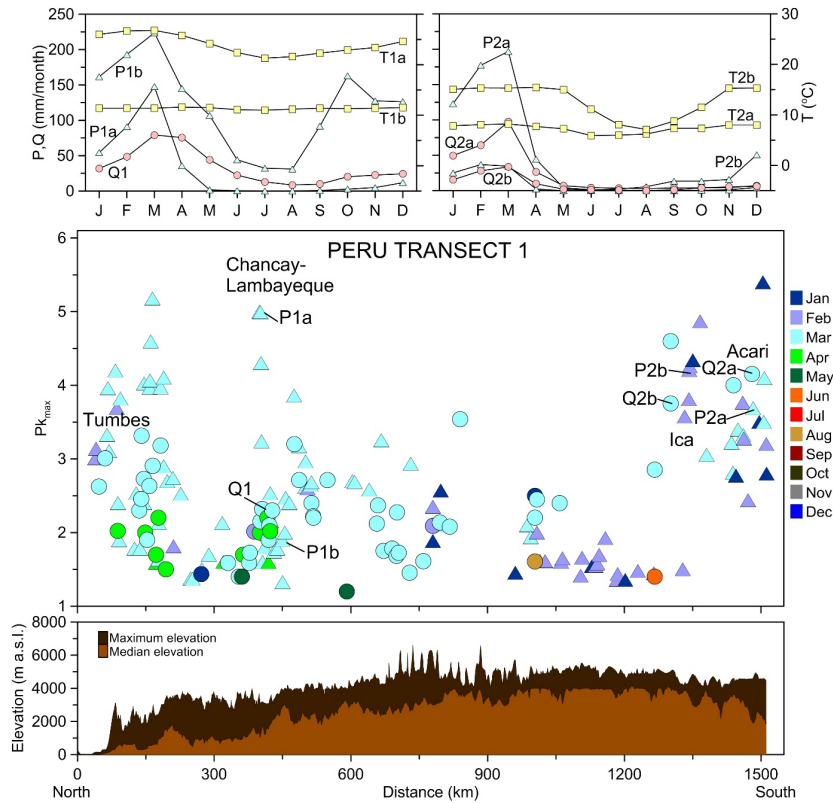


**Fig. 2.** Top: Long term water balances for the Chancay-Lambayeque basin (2400 km<sup>2</sup>) (left), and the Ica (2b) (2600 km<sup>2</sup>) and Acari (2a) (250 km<sup>2</sup>) basins (right). Precipitation (triangles), runoff depths (circles) and air temperatures (squares). Middle: Maximum seasonality strength  $Pk_{max}$  and month of occurrence along Transect 1 (Peru) for precipitation (triangles) and for runoff (circles). Bottom: median and maximum elevations of the transect.

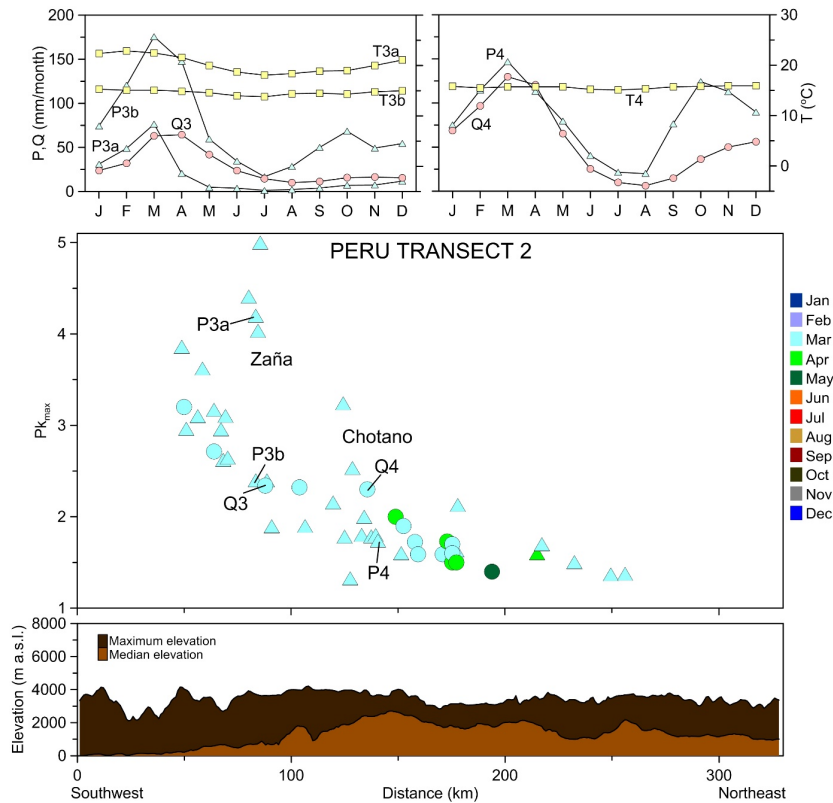


**Fig. 3.** Top: Long term water balances for the Zaña basin (673 km<sup>2</sup>) (left) and the Chotano basin (356 km<sup>2</sup>) (right). Precipitation (triangles), runoff depths (circles) and air temperatures (squares). Middle: Maximum seasonality strength  $Pk_{max}$  and month of occurrence along Transect 2 (Peru) for precipitation (triangles) and for runoff (circles). Bottom: median and maximum elevations of the transect. Note that, inside a basin, the Maximum Pardé coefficients  $Pk_{max}$  of runoff (circles) are smaller than those of precipitation (triangles) in the Southwest (Pacific basins) and greater than those of precipitation in the Northeast (Atlantic basins).

The maxima of mean monthly precipitation generally occur in summer from June to August. The exception is the very South of the transect where they tend to occur in November (Fig. 4). The latter values are due to weather patterns from the Mediterranean which tend to bring moist air to the Alps when the Mediterranean Sea surface is still warm, so can transfer moisture and energy to the atmosphere. Their influence only extends to the southernmost part of the Alps.

The runoff seasonality shows a more heterogeneous pattern than that of precipitation. In the northern lowlands (km 0–100)  $Q-Pk_{max}$  mean value is 1.5 and the maxima occur in March. In the High Alps in the middle of the transect, the  $Q-Pk_{max}$  are significantly higher (mean value is 2.2) and the maxima occur in April, May and June. Finally, in the South,  $Q-Pk_{max}$  are between 1.2 and 1.6 (mean value is 1.4) and the maxima occur in either April-May or November. The Maximum Pardé coefficients  $Pk_{max}$  of runoff (circles in Fig. 4) are almost always greater than those of precipitation (triangles), particularly in the high mountains.

The water balance for the Mattig Basin (Fig. 4 top left) in the Northern lowlands of Austria shows that, although precipitation occurs throughout the year, it is summer dominated from June to August. This is also the time when the maximum evaporation occurs as indicated by the strong seasonality of air temperature. The strong seasonality of evaporation that is in phase with that of precipitation (Sivapalan et al., 2005) results in a very uniform runoff regime throughout the year and there-

fore a slightly smaller  $Q-Pk_{max}$  (1.3) than  $P-Pk_{max}$  (1.4). This is typical of the lowlands in the region (Parajka et al., 2009). The runoff shows a small peak in March when the soils are still wet, so runoff coefficients are higher than in summer.

The Alpine areas show quite a contrasting behaviour as illustrated by the Enns basin (Fig. 4 top right). The precipitation regime is similar to Mattig, but evaporation contributes less to the water balance due to lower temperatures in the higher elevations. Even more importantly, snow storage and snow melt play a clear role. The runoff maxima occur in May as a result of snow melt. Runoff is relatively low in December and January due to snow storage. This explains the fact that  $Q-Pk_{max}$  (2.0) is greater than  $P-Pk_{max}$  (1.7) in this basin. There are catchments that are located at higher elevations than the Enns basin and these exhibit even higher  $Q-Pk_{max}$  (up to 3) due to the stronger effect of snow melt and storage on the water balance. Runoff seasonalities larger than precipitation seasonalities are typical of many regions around the world where the runoff regime is dominated by snowmelt (Dettinger and Diaz, 2000).

In the very South of Transect 3, precipitation is bimodal (not shown in the figure) and similarly the runoff regime is bimodal with a main maximum in May and a secondary maximum in November. The May maximum is related to snow melt, the November maximum is related to the precipitation maximum. One basin on Transect 3 (at km 255) in fact shows the main runoff maximum in November.

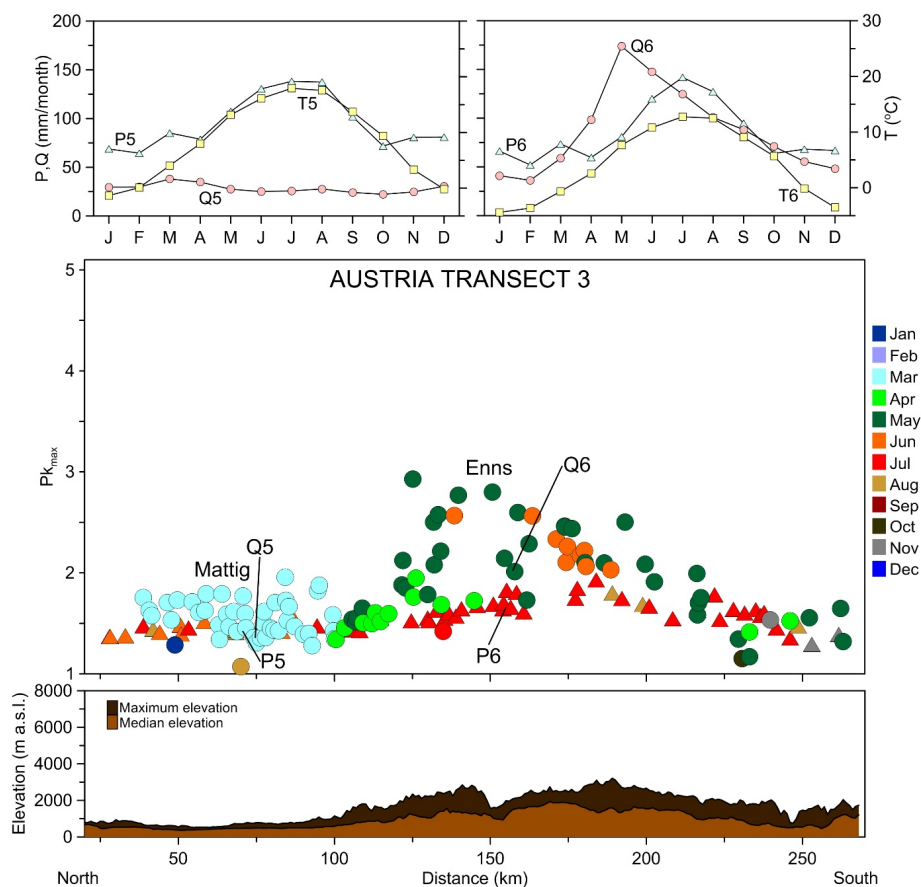


**Fig. 4.** Top: Long term water balances for the Mattig basin (447 km<sup>2</sup>) (left) and the Enns basin (649 km<sup>2</sup>) (right). Precipitation (triangles), runoff depths (circles) and air temperatures (squares). Middle: Maximum seasonality strength  $Pk_{max}$  and month of occurrence along Transect 3 (Austria) for precipitation (triangles) and for runoff (circles). Bottom: median and maximum elevations of the transect. Note that the Maximum Pardé coefficients  $Pk_{max}$  of runoff (circles) are almost always greater than those of precipitation (triangles), particularly in the high mountains.

### Controls on the seasonality of runoff and of precipitation in the Austrian and Peruvian transects

While the transects in Figs. 2–4 have highlighted the seasonality with respect to mountain ranges and atmospheric moisture fluxes, it is also useful to explicitly analyse the seasonality with respect to climate. Five Köppen climate groups were identified for the Peruvian transects, and two groups for the Austrian transect.

The Peruvian Pacific lowlands are characterized by desert and arid climates (P1a and P3a) with precipitation from 0 to 300 mm/yr per year, where rainfall tends to occur as discrete and intense events (Takahashi, 2004). Steppe and temperate climates with dry winters are found in the Peruvian Pacific highlands with Atlantic influence (P3b and P1b), and steppe and hemi-boreal climates are found in the Peruvian Pacific highlands with Pacific influence (P2b, P2a).

Transect 3 in Austria shows two main climates: temperate in the lowlands (P5) and snow dominated in the highlands or Alps (P6). The comparison between the Peruvian and Austrian transects indicates that the variability of the strength of seasonality in Austria is much more limited than that in Peru. This is due to

the more limited range of climate zones in Austria. Table 2 shows the ranges of the maximum strength of seasonality. Because of the different latitudes, the snow dominated regimes in Peru are found above around 4000 m a.s.l., while in Austria above around 600 m a.s.l. Interestingly, the strength of seasonality of monthly precipitation in snow dominated region is very similar in both countries. This indicates that monthly precipitation regime in these regions has not very strong seasonality ( $P-Pk_{max}$  is in range between 1.4 and 1.8). The somewhat weaker seasonality of monthly runoff in snow dominated Austrian basins is likely caused by their lower elevation. In many basins, the main snowmelt runoff season occurs earlier than monthly precipitation maxima in summer, so the seasonality of runoff regime is less strong.

Fig. 5 shows the relationship between  $P-Pk_{max}$  and  $Q-Pk_{max}$  stratified by the Köppen climate classes for the three transects. Overall,  $P-Pk_{max}$  decreases from tropical savanna climate (Fig. 5 top left) to snow dominated climate (Fig. 5 bottom right). For the desert climate and the semi-arid steppe climate,  $Q-Pk_{max}$  is smaller than  $P-Pk_{max}$  while for the snow dominated climate it is bigger. The other climate zones show a more mixed pattern.

**Table 2.** Ranges of the strength of seasonality of precipitation ( $P-Pk_{max}$ ) and runoff ( $Q-Pk_{max}$ ) for Transects 1 and 2 (Peru) and Transect 3 (Austria) according to the climate classifications of Fig. 5.

Country	Climate	Köppen class	$P-Pk_{max}$ range		$Q-Pk_{max}$ range	
			min	max	min	max
Peru	Tropical	Aw	3.7	5.2	2.5	3.0
	Semiarid	BS	2.4	4.1	2.0	3.0
	Desert	BW	3.2	5.0	2.0	3.2
	Temperate	CW	1.5	3.1	1.4	3.2
	Hemiboreal	Dwb	1.4	3.7	1.5	4.2
Austria	Snow dominated	E	1.4	1.7	2.4	2.5
	Temperate	CW	1.4	1.8	1.2	2.2
	Snow dominated	E	1.5	1.9	1.5	2.4

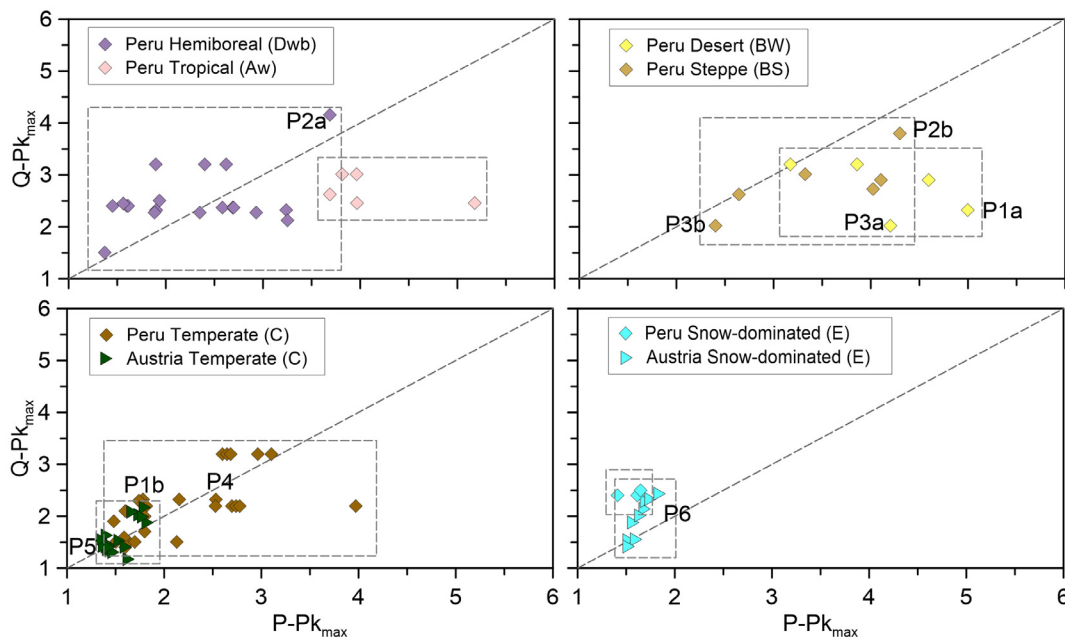


**Fig. 5.** Relationship between maximum seasonality index of precipitation  $P-Pk_{max}$  and runoff  $Q-Pk_{max}$  stratified by Köppen climate classes for Peru and Austria: Labels refer to the example stations of Figs. 2–4.

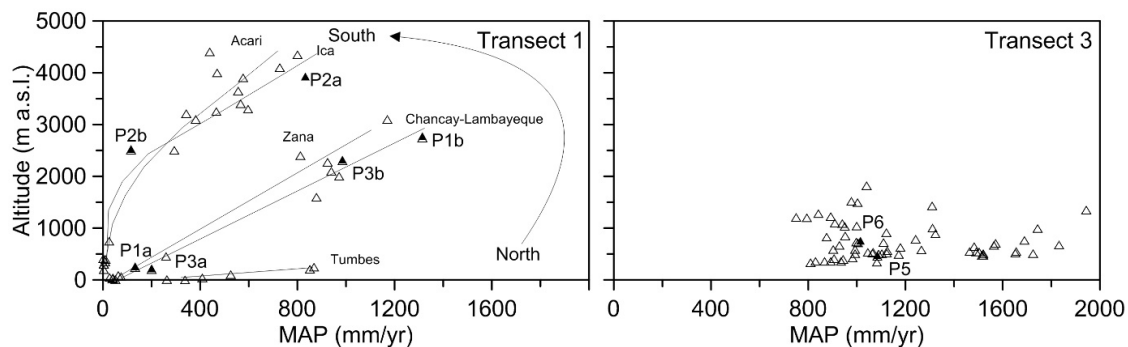


**Fig. 6.** Relationship between mean annual precipitation (MAP) and altitudes of the precipitation stations in the Peruvian Transect 1 (left) and Austrian Transect 3 (right). Lines link the stations inside of five Peruvian basins (Tumbes, Chancay-Lambayeque, Zaña, Ica and Acari).

In order to put the seasonalities into context, Fig. 6 shows mean annual precipitation plotted versus station altitude. In the Peruvian transects, MAP increases clearly with altitude. In the North of Transect 1 (Tumbes basin) the increase is large with stations at 250 m a.s.l. exhibiting 868 mm/yr. The gradient becomes gradually flatter (smaller altitudinal dependence of MAP) as one moves to the South. Acari, located in the South of Transect 1, has the same MAP for stations at an elevation of 4500 m a.s.l. Although stations P3b and P2b have similar altitudes and steppe climates, the stronger Atlantic influence is reflected in significantly larger MAP and lower strength of seasonality of precipitation in P3b.

Transect 3 (Fig. 6 right) shows that the altitudinal effect on MAP in Austria is much less pronounced than in Peru. It appears that MAP is more affected by the location relative to the Alpine range than altitude per se, as the largest MAP occurs at the northern (windward) fringe of the Alps rather than the highest mountain tops. The latter exhibit less MAP as much of the moisture has already precipitated at the time the air masses arrive at the main ridge of the Alps. Fig. 6 also clearly illustrates that the Austrian transect (Transect 3) overall is much wetter than the Peruvian transects.

### Seasonality of annual maximum daily precipitation and annual maximum daily runoff along transects

The concentration of the seasonal occurrence of annual maximum daily precipitation and runoff (i.e. floods) along the three transects is presented in Figs. 7, 8 and 9. In each of the figures, the top panel shows the concentration index  $r$  of extreme precipitation (triangles) and floods (circles) along the distance of the transect. To understand how the extreme events are related to the monthly regime, the difference in the occurrence of extreme events and seasonal monthly maximum (month of  $Pk_{max}$ , represented as the middle of month) is colour coded. The yellow-red colours indicate earlier occurrence of extreme events, blue colour shows later floods or extreme precipitation relative to the occurrence of monthly maxima. The size of the symbols indicates the strength of monthly runoff or precipitation seasonality.

The Pacific Transect 1 (Fig. 7) shows a clear link between the strength of the monthly regime and extreme events. The parts of the transect with strong monthly seasonality of runoff and precipitation have also the extreme events concentrated along the same date. The concentration index  $r$  of extreme precipitation of Transect 1 (Fig. 7) is particularly large in the North and South of the transect. While the annual maximum daily precipitation in the North tends to occur in February and March, in the southern part of the transect it tends to occur earlier – in January and February. A larger variability in the

occurrence of extreme precipitation is observed in the Chancay (120–140 km), Alto Marañon, and Jequetepeque regions (around 400–520 km). In the Chancay region the  $r$  index varies between 0.1 and 0.8 and the seasonal precipitation maximum ( $P-Pk_{max}$ ) tends to be lower than 2.0. The mean date of extreme precipitation occurs 1–2 months earlier than the seasonal precipitation maxima. In the Alto Marañon region, the mean date of occurrence is in January, but the concentration index is smaller than 0.4. In contrast, the annual maximum daily precipitation is much more concentrated ( $r > 0.7$ ) in the Jequetepeque region and it occurs mostly in February. A comparison with the gradient of mean annual precipitation along the Pacific coast in Lavado et al. (2012) indicates that the decrease in mean annual precipitation from North to South does not have a large effect on the concentration of maximum daily precipitation events. The most dominant factor controlling extreme precipitation at or near equatorial areas is the Southern Oscillation (Goldberg et al., 1987; Kane, 1999; Rossel and Cadier, 2009), which regulates the atmospheric circulation regimes responsible for moisture inflow from the Pacific Ocean to the Peruvian basins. The timing and intensity of strong anomalies in moisture inflow are connected to flood-generating storms (Craig and Shimada, 1986; Waylen and Laporte, 1999; Waylen and Poveda, 2002), especially in basins where orographic effects condensate the anomalous precipitable water leading to extreme precipitation events. The orographic influence is, however, nonlinear and monotonic, since precipitation increases with elevation up to a certain extent, beyond which it actually decreases due to the progressive lack of precipitable water (Perdigão and Blöschl, 2014).

The trend of the concentration index of flood events (circles, Fig. 7) follows the variability of extreme precipitation. The Pacific North of the transect is characterized by larger  $r$  values for basins with stronger monthly runoff regimes (i.e. larger  $Q-Pk_{max}$ ). For example, in the Tumbes basin, the floods occur in February and the  $r$  index is larger than 0.7. In the Chamaya region (190–420 km), the floods typically occur between December and March, but the variability of the concentration index varies between 0.2 and 0.8. In the South (Ica and Acari regions), the floods are much more concentrated and occur in February and March. Similarly as for annual maximum daily precipitation, there is no clear pattern between the variability of the concentration index of floods and the variability of specific runoff presented in Lavado et al. (2012). Indeed, the relationship between specific runoff and latitude is not as regular as the decrease of mean annual precipitation along the Pacific transect. Moreover, the variability of concentration index is affected by the impact of El Niño and La Niña events. The Southern Oscillation is linked to the Pacific Ocean circulation and

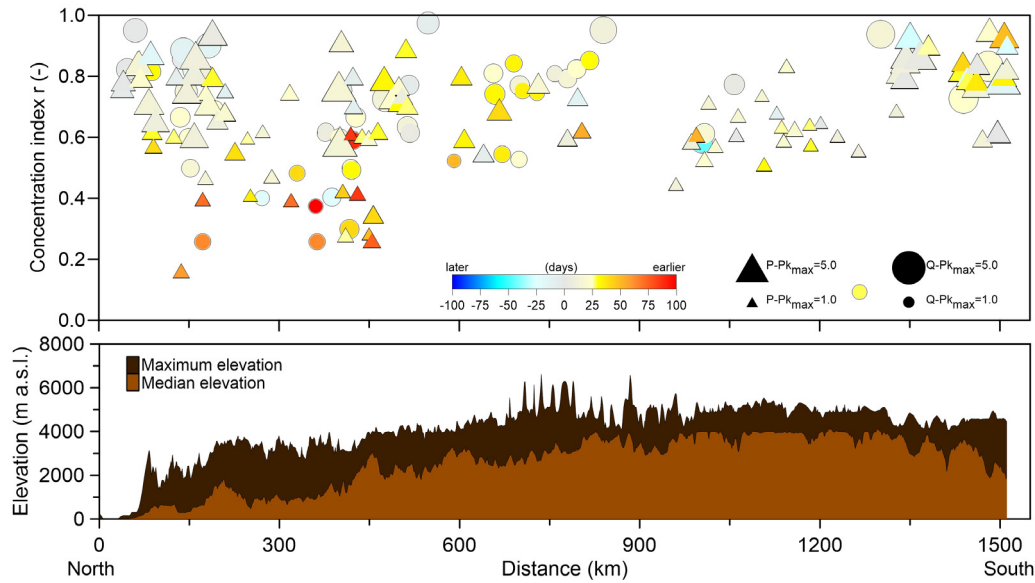


**Fig. 7.** Seasonality concentration index of annual maximum daily precipitation (triangles) and floods (circles) along Transect 1 (Peru). Colours indicate whether floods (or precipitation events) occur later or earlier than mid of month of the respective maximum Parde coefficients ( $Pk_{max}$ ). Bottom: median and maximum elevations of the transect.

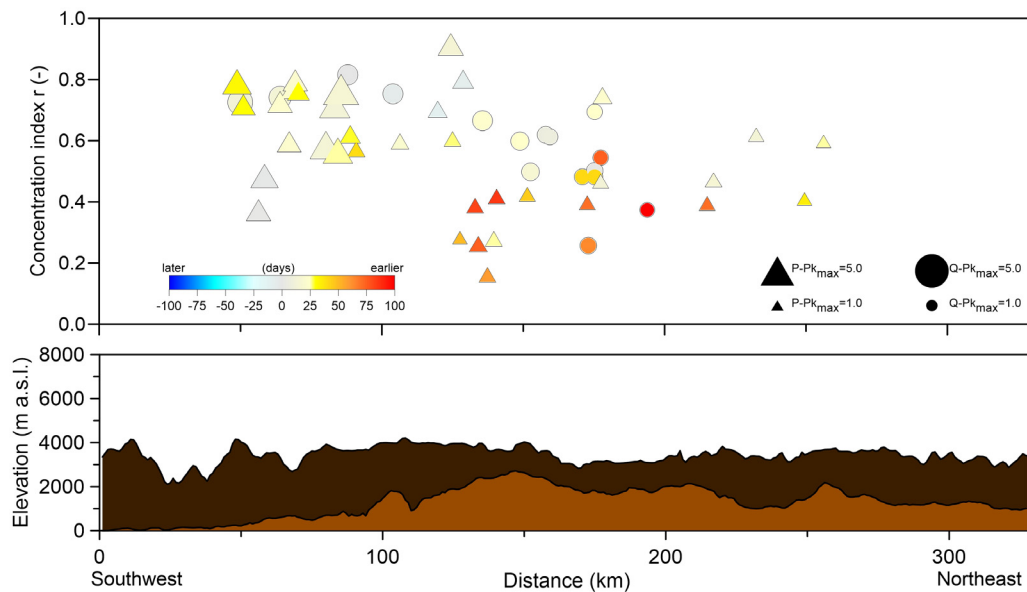


**Fig. 8.** Seasonality concentration index of annual maximum daily precipitation (triangles) and floods (circles) along Transect 2 (Peru). Colours indicate whether floods (or precipitation events) occur later or earlier than mid of month of the respective maximum Parde coefficients ( $Pk_{max}$ ). Bottom: median and maximum elevations of the transect.

regulates the strength of westward moisture fluxes, especially within inter tropical latitudes (Cushman-Roisin, 1994; Holton, 1992). When the westward fluxes weaken, net warming and mass accumulation over the coastal areas in South America leads to El Niño anomalies causing an increase of oceanic evaporation and hence the moisture inflow with an anomalous amount of precipitable water (Cushman-Roisin, 1994; Holton, 1992). Such events increase the strength of seasonality indicators in near-equatorial basins with strong Pacific influence. An opposite case is observed during the La Niña anomaly, which increases the precipitation deficit in near-equatorial regions and southern part of the transect.

Transect 2 (Fig. 8) clearly shows that the extreme precipitation events in the Pacific part of the transect (0–130 km) are

more seasonally concentrated (mean  $r$  value is 0.67) than the events in regions with Atlantic influence (mean  $r$  value less than 0.45). The mean date of extreme precipitation in the Pacific part tends to occur in February which is typically the same season as the month of  $P-Pk_{max}$ . In the Atlantic part, however, the mean date of extreme precipitation is in January, which is 1–2 months earlier than the monthly precipitation maximum. The same pattern is observed for the concentration of floods. Larger  $r$  values are observed in the Pacific part of the transect and the mean date of floods tends to occur within the month of monthly runoff maxima. In the Atlantic part, the  $r$  value of floods is lower, so the floods tend to occur in different seasons. The mean date of flood occurrence tends to be 1–2 months earlier than the occurrence of monthly runoff maxima.

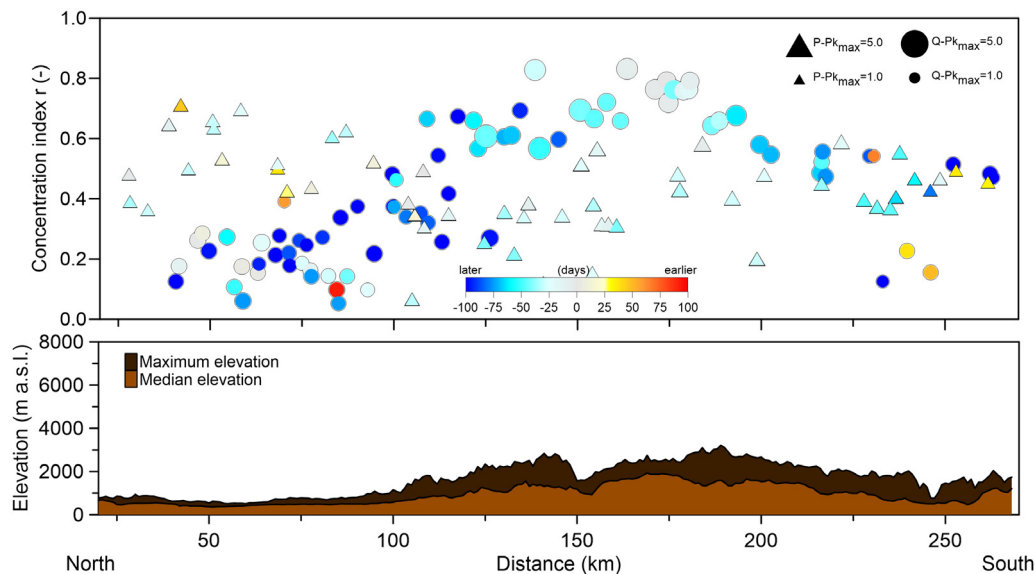


**Fig. 9.** Seasonality concentration index of annual maximum daily precipitation (triangles) and floods (circles) along Transect 3 (Austria). Colours indicate whether floods or precipitation events occur later or earlier than mid of month of the respective maximum Parde coefficients ( $Pk_{max}$ ). Bottom: median and maximum elevations of the transect.

Transect 3 across Austria (Fig. 9) suggests that the concentration of extreme precipitation events is generally larger in the northern lowlands than in the alpine part of the transect. In the mountains the extreme precipitation events tend to occur in August, which is about 2 months later than the monthly precipitation maxima. As indicated in Parajka et al. (2008, 2009), the northern fringe of the Central Alps shows very small  $r$  values ( $r < 0.2$ ), which is likely caused by orographic rainfall occurring throughout the year. In the southern part of the transect precipitation maxima occur in autumn which is related to the characteristic weather patterns of this region.

The seasonality and concentration of the flood events along the transect (Fig. 9) show opposite trends in comparison with extreme precipitation. The largest  $r$  values are observed in the alpine (central) part of the transect, where  $r$  tends to be larger than 0.7. The floods here tend to occur in the same season as monthly runoff maxima. The summer floods in the Alps are controlled mainly by the large snow storage and melt component combined with the seasonality of extreme precipitation. In the northern lowland part (Innviertel region), the concentration index is lower and does not exceed 0.4. In this part of the transect the floods tend to occur in summer, i.e. about 3 months later than maximum monthly runoff. The flood seasonality here is controlled mainly by summer extreme precipitation and larger soil moisture. The southern part of the transect (Eastern Carinthia) exhibits a particular flood behaviour. As indicated in Parajka et al. (2009), the seasonality of monthly runoff is similar to that of other regions of the same altitude, but the seasonality of mean monthly precipitation, annual maximum daily precipitation and annual maximum daily floods are very different. Parajka et al. (2009) suggest that this region is climatologically and hydrologically different from the rest of Austria. Indeed, weather patterns from the south are known to cause floods in this part of transect in autumn which is controlled by lower evaporation and higher soil moisture in autumn.

## CONCLUSIONS

The analyses of precipitation and runoff data along topographic gradients in Peru and Austria showed that, overall, in Peru the spatial variation in seasonality is much larger than in

Austria. This is because of the larger diversity in climate and topography. In the Atlantic influenced Peruvian basins and most Austrian basins the strength of the seasonality of runoff is greater than that of precipitation. In Peru this is because evaporation is rather uniformly distributed throughout the year, which reduces the mean more than the amplitude. In most of the Austrian basins, snowmelt increases runoff seasonality relative to that of precipitation. In the Pacific influenced Peruvian basins, the strength of the seasonality of runoff is mostly smaller than that of precipitation at the coast which is due to the more uniform precipitation in the mountainous headwaters of these basins. The present analyses could be expanded by studying the dynamics of the water balance components in more detail, in particularly the role of catchment storage on the seasonality of runoff.

*Acknowledgements.* The authors would like to thank the Austrian Science Foundation (FWF Project no. P 23723- N21) and the Flood Change project of the ERC for financial support. The authors would also like to acknowledge the Peruvian National Meteorology and Hydrology Service (SENAMHI) and the Austrian Hydrographic Service (HZB) for providing hydrological data.

## REFERENCES

- Bayliss, A.C., Jones, R.C., 1993. Peaks-over-threshold flood database: Summary statistics and seasonality. IH Report No. 121. Institute of Hydrology, Walingford, UK.
- Blöschl, G., Sivapalan, M., Wagener, T., Viglione, A., Savenije, H. (Eds.), 2013. Runoff Prediction in Ungauged Basins - Synthesis across Processes, Places and Scales. Cambridge University Press, Cambridge, UK.
- Bower, D., Hannah, D.M., McGregor, G.R., 2004. Techniques for assessing the climatic sensitivity of river flow regimes. *Hydrological Processes*, 18, 2515–2543.
- Burn, D.H., 1997. Catchment similarity for regional flood frequency analysis using seasonality measures. *Journal of Hydrology*, 202, 212–230.
- Craig, A.K., Shimada, I., 1986. El Niño flood deposits at Batán Grande, northern Peru, *Geochronology*, 1, 29–38.

- Cushman-Roisin, B., 1994. Introduction to Geophysical Fluid Dynamics. Prentice Hall, 320 pp.
- Dettinger, M.D., Diaz, H.F., 2000. Global characteristics of stream flow seasonality and variability. *Journal of Hydrometeorology*, 1, 289–310.
- Espinoza Villar, J.C., Ronchail, J., Guyot, J.L., Ronchail, J., Naziano, F., Lavado, W., De Oliveira, E., Pombosa, R., Vauchel, P., 2009. Spatio-temporal rainfall variability in the Amazon Basin Countries (Brazil, Peru, Bolivia, Colombia and Ecuador). *International Journal of Climatology*, 29, 1574–1594.
- Falkenmark, M., Chapman, T. (Eds.), 1989. Comparative Hydrology: an Ecological Approach to Land and Water Resources. Unesco, Paris.
- Fenicia, F., Kavetski, D., Savenije, H.H.G., Clark, M.P., Schoups, G., Pfister, L., Freer, J., 2013. Catchment properties, function, and conceptual model representation: is there a correspondence? *Hydrological Processes*, 28, 4, 2451–2467. DOI: 10.1002/hyp.9726.
- Gaál, L., Szolgay, J., Kohnová, S., Parajka, J., Merz, R., Viglione, A., Blöschl, G., 2012. Flood timescales: Understanding the interplay of climate and catchment processes through comparative hydrology. *Water Resources Research*, 48, W04511. DOI: 10.1029/2011WR011509.
- Goldberg, R.A., Tisnado, G., Scofield, R.A., 1987. Characteristics of extreme rainfall events in northwestern Peru during the 1982–1983 El Niño period. *Journal of Geophysical Research: Oceans*, 92, C13, 14225–14241.
- Gottschalk, L., 1985. Hydrological regionalization of Sweden. *Hydrological Sciences Journal*, 30, 1, 65–83.
- Gupta, H.V., Perrin, C., Blöschl, G., Montanari, A., Kumar, R., Clark, M., Andréassian, V., 2014. Large-sample hydrology: a need to balance depth with breadth. *Hydrology and Earth System Sciences*, 18, 463–477. DOI: 10.5194/hess-18-463-2014.
- Haines, A.T., Finlayson, B.L., McMahon, T.A., 1988. A global classification of river regimes. *Applied Geography*, 8, 255–272.
- Holton, J.R., 1992. An Introduction to Dynamic Meteorology. Academic Press, 511 pp.
- Johnston, C.A., Shmagin, B.A., 2008. Regionalization, seasonality, and trends of streamflow in the U.S. Great Lakes Basin. *Journal of Hydrology*, 362, 69–88.
- Kane, R.P., 1999. El Niño / La Niña relationship with rainfall at Huancayo, in the Peruvian Andes. *International Journal of Climatology*, 20, 63–72.
- Köppen, W., 1884. Die Wärmezonen der Erde, nach der Dauer der heissen, gemässigten und kalten Zeit und nach der Wirkung der Wärme auf die organische Welt betrachtet. *Meteorologische Zeitschrift*, 1, 215–226.
- Krasovskaia, I., 1995. Quantification of the stability of river flow regimes. *Hydrological Sciences Journal*, 40, 5, 587–598.
- Krasovskaia, I., 1996. Sensitivity of the stability of river flow regimes to small fluctuations in temperature. *Hydrological Sciences Journal*, 41, 2, 251–264.
- Krasovskaia, I., Gottschalk, L., 2002. River flow regimes in a changing climate. *Hydrological Sciences Journal*, 47, 4, 597–609.
- Lagos, P., Silva, Y., Nickl, E., Mosquera, K., 2008. El Niño – related precipitation variability in Perú. *Advances in Geosciences*, 14, 231–237. DOI: 10.5194/adgeo-14-231-2008.
- Lavado Casimiro, W.S., Ronchail, J., Labat, D., Espinoza, J.C., Guyot, J.L., 2012. Basin-scale analysis of rainfall and runoff in Peru (1969–2004): Pacific, Titicaca and Amazonas watersheds. *Hydrological Sciences Journal*, 57, 4, 1–18.
- Merz, R., Blöschl, G., 2003. A process typology of regional floods. *Water Resources Research*, 39, 12, 1340. DOI: 10.1029/2002WR001952.
- Merz, R., Piock-Ellena, U., Blöschl, G., Gutknecht, D., 1999. Seasonality of flood processes in Austria. In: Gottschalk, L., Olivry, J.-C., Reed, D., Rosbjerg, D. (Ed.): *Hydrological Extremes: Understanding, Predicting, Mitigating*. Wallingford, UK: IAHS Press, 273–278.
- MINEDU, 2008. Guía de aplicación de arquitectura bioclimática en locales educativos. Ministerio de Educación del Perú, Lima-Perú. IN070117ME
- Molnar, P., Burlando, P., 2008. Variability in the scale properties of high-resolution precipitation data in the Alpine climate of Switzerland. *Water Resources Research*, 44, W10404. DOI: 10.1029/2007WR006142.
- Montanari, A., Young, G., Savenije, H.H.G., Hughes, D., Wagener, T., Ren, L.L., Koutsoyiannis, D., Cudennec, C., Toth, E., Grimaldi, S., Blöschl, G., Sivapalan, M., Beven, K., Gupta, H., Hipsey, M., Schaeffli, B., Arheimer, B., Boegh, E., Schymanski, S.J., Di Baldassarre, G., Yu, B., Hubert, P., Huang, Y., Schumann, A., Post, D., Srinivasan, V., Harman, C., Thompson, S., Rogger, M., Viglione, A., McMillan, H., Characklis, G., Pang, Z., Belyaev, V., 2013. “Panta Rhei – Everything Flows”: Change in hydrology and society – The IAHS Scientific Decade 2013–2022. *Hydrological Sciences Journal*, 58, 1256–1275.
- Parajka, J., Merz, R., Szolgay, J., Blöschl, G., Kohnová, S., Hlavčová, K., 2008. A comparison of precipitation and runoff seasonality in Slovakia and Austria. *Meteorological Journal*, 11, 9–14.
- Parajka, J., Kohnová, S., Merz, R., Szolgay, J., Hlavčová, K., Blöschl, G., 2009. Comparative analysis of the seasonality of hydrological characteristics in Slovakia and Austria. *Hydrological Sciences Journal*, 54, 3, 456–473.
- Parajka, J., Kohnová, S., Bálint, G., Barbuc, M., Borga, M., Claps, P., Cheval, S., Dumitrescu, A., Gaume, E., Hlavčová, K., Merz, R., Pfaundler, M., Stancalie, G., Szolgay, J., Blöschl, G., 2010. Seasonal characteristics of flood regimes across the Alpine-Carpathian range. *Journal of Hydrology*, 394, 1–2, 78–89.
- Pardé, M., 1947. *Fleuves et rivières*. Colin, Paris, France.
- Perdigão, R.A.P., Blöschl, G., 2014. Spatiotemporal flood sensitivity to annual precipitation: Evidence for landscape-climate coevolution. *Water Resources Research*, 50, 5492–5509. DOI: 10.1002/2014WR015365.
- Petrow, Th., Merz, B., Lindenschmidt, K.-E., Thielen, A.H., 2007. Aspects of seasonality and flood generating circulation patterns in a mountainous catchment in south-eastern Germany. *Hydrology and Earth System Sciences*, 11, 1455–1468.
- Piock-Elena, U., Pfaundler, M., Blöschl, G., Burlando, P., Merz, R., 2000. Saisonalitätsanalyse als Basis fuer die Regionalisierung von Hochwaessern in Oesterreich und der Schweiz. *Wasser, Energie, Luft*, 92, 1/2, 13–21.
- Poveda, G., Waylen, P.R., Pulwarty, R.S., 2006. Annual and inter-annual variability of the present climate in northern South America and southern Mesoamerica. *Palaeogeography, Palaeoclimatology, Palaeoecology*, 234, 1, 3–27.
- Rau, P., Condom, T., 2010. Spatio-temporal analysis of rainfall in the mountain regions of Peru (1998–2007). *Revista Peruana Geo-Atmosférica RPGA*, 2, 16–29. Available from: [http://www.senamhi.gob.pe/rpga/pdf/2010\\_vol02/art2.pdf](http://www.senamhi.gob.pe/rpga/pdf/2010_vol02/art2.pdf).
- Rossel, F., Cadier, E., 2009. El Niño and prediction of anomalous monthly rainfalls in Ecuador. *Hydrological Processes*, 23, 3253–3260.

- Sauquet, E., Gottschalk, L., Krasovskaia, I., 2008. Estimating mean monthly runoff at ungauged locations: an application to France. *Hydrology Research*, 39, 5–6, 403–423.
- Sivapalan, M., Blöschl, G., Merz, R., Gutknecht, D., 2005. Linking flood frequency to long-term water balance: Incorporating effects of seasonality. *Water Resources Research*, 41, W06012. DOI: 10.1029/2004WR003439.
- Takahashi, K., 2004. The atmospheric circulation associated with extreme rainfall events in Piura, Peru, during the 1997–1998 and 2002 El Niño events. *Annales Geophysicae*, 22, 3917–3926.
- UNESCO, 2006. Balance hídrico superficial del Perú a nivel multianual. Uruguay: PHILAC, Documentos Técnicos del PHI-LAC, N°1.
- Vera, H., Acuña, J., Yerrén, J., 2000. Balance hidrico superficial de las cuencas de los rios Tumbes y Zarumilla. Lima, Dirección General de hidrología y Recursos Hídricos-Senamhi. Available from [http://www.senamhi.gob.pe/pdf/estudios/Paper\\_BHSTUZA.pdf](http://www.senamhi.gob.pe/pdf/estudios/Paper_BHSTUZA.pdf)
- Wagener, T., Sivapalan, M., Troch, P., Woods, R., 2007. Catchment classification and hydrologic similarity. *Geography Compass*, 1, 901–931.
- Waylen, P., Laporte, M.S., 1999. Flooding and the El Niño–Southern Oscillation phenomenon along the Pacific coast of Costa Rica. *Hydrological Processes*, 13, 16, 2623–2638.
- Waylen, P., Poveda, G., 2002. El Niño–Southern Oscillation and aspects of western South American hydro-climatology. *Hydrological Processes*, 16, 6, 1247–1260.

Received 10 October 2016

Accepted 8 December 2016